UNIVERSITAT POLITÈCNICA DE VALÈNCIA

Escola Tècnica Superior d'Enginyeria Agronòmica i del Medi Natural

UNIVERSITAT POLITÈCNICA DE VALÈNCIA

School of Agricultural Engineering and Environment

Real-time PCR quantification of muscular atrophy markers in the presence of sphingolipid metabolism inhibitors.

End of Degree Project

Bachelor's Degree in Biotechnology

AUTHOR: Candela Candela, Alba María

Tutor: García Gimeno, María Adelaida

Experimental director: MEACCI, ELISABETTA

ACADEMIC YEAR: 2021/2022

UNIVERSITAT POLITÈCNICA DE VALÈNCIA

ESCOLA TÈCNICA SUPERIOR D'ENGINYERIA AGRONÒMICA I DEL MEDI NATURAL (ETSIAMN)

UNIVERSITÀ DEGLI STUDI DI FIRENZE

DIPARTIMENTO DI SCIENZE BIOMEDICHE SPERIMENTALI E CLINICHE «MARIO SERIO» - UNIT OF MOLECULAR AND APPLIED BIOLOGY

Real-time PCR quantification of muscular atrophy markers in the presence of sphingolipid metabolism inhibitors

Bachelor's Degree in Biotechnology

End of Degree Project

Author: Alba María Candela Candela

Tutors:

María Adelaida García Gimeno

Prof. Elisabetta Meacci

Academic Year: 2021/2022

Valencia, September 2022

Real-time PCR quantification of muscular atrophy markers in the presence of sphingolipid metabolism inhibitors

Abstract

Skeletal muscle wasting can be caused in several pathological conditions leading to an imbalance between protein synthesis and degradation and activating a whole set of signalling pathways which result in the activation of atrophy-related genes, such as Atrogin-1 or MuRF-1 and thus in muscle atrophy and cancer-associated cachexia. This protein dysregulation can be produced by a variety of stimuli, including upregulated levels of molecules like ubiquitin ligases, glucocorticoids or inflammation factors like Tumour Necrosis Factor TNFα. Sphingosine 1-phosphate is a bioactive sphingolipid that has been linked to crucial cellular processes and functions through the specific binding to its receptors (S1PR1-5). Enzymes and compounds, such as kinases (SphK1 and SphK2) or transporters (Snps2), from its metabolism have been proposed as an important part of atrogene activation pathways, still not fully understood. Moreover, they have been also noted to interact with histone deacetylases (HDACs) in the nucleus, which importance lies in the fact that acetylation/deacetylation processes are key to initiate gene transcription.

The aim of this study is to expand the knowledge of this S1P/SphK axis and its role in skeletal muscle atrophy. For that purpose, cultures of murine C2C12 cells were used as myoblasts, committed precursors; and myotubes, fully differentiated cells; to mimic cancer-associated cachexia conditions by the use of Dexamethasone, a synthetic glucocorticoid. Afterwards, cell cultures were treated with an inhibitor of histone deacetylase (Trichostatin A) that has been related to improvements in preventing and regeneration skeletal muscle atrophy.

Variation on gene expression levels of SphK1, SphK2, p21 and Atrogin-1 was evaluated by reverse transcription and real-time PCR. The results indicated a general decrease in the levels of expression in myoblasts, while showing a significant increase in DEXA-treated myotubes, further reduced by TSA treatment and validating the important role of HDAC pathways.

Key words: *skeletal muscle; muscular atrophy; sphingolipids; real-time PCR*

Author: Alba María Candela Candela

Academic Tutor: Dña. María Adelaida García Gimeno

Co-tutor: Dña. Elisabetta Meacci

Valencia, September 2022

Cuantificación mediante real time PCR de marcadores de atrofia muscular en presencia de inhibidores del metabolismo de esfingolípidos

Resumen

La pérdida de músculo esquelético puede ser consecuencia de varias condiciones patológicas que conducen a un desequilibrio entre la síntesis y la degradación de las proteínas y a la activación de todo un conjunto de vías de señalización que desembocan en la activación de genes relacionados con la atrofia, como el Atrogin-1 o el MuRF-1 y, por tanto, en la atrofia muscular y la caquexia asociada al cáncer. Esta incorrecta regulación proteica puede ser producida por una variedad de estímulos, incluyendo sobreexpresión de moléculas como la ubiquitina ligasas, glucocorticoides o factores de inflamación, como el factor de crecimiento tumoral TNFα. La esfingosina 1-fosfato es un esfingolípido bioactivo que se ha relacionado con procesos y funciones celulares cruciales mediante la unión específica a sus receptores (S1PR1-5). Se ha propuesto que las enzimas y los compuestos, como las quinasas (SphK1 y SphK2) o los transportadores (Snps2), de su metabolismo son una parte importante de las vías de activación de los *atrogenes*, cuyo funcionamiento aún no se conocen por completo. Además, también se ha observado que interactúan con las histonas deacetilasas (HDACs) en el núcleo, cuya importancia radica en que los procesos de acetilación/deacetilación son clave para iniciar la transcripción génica.

El objetivo de este estudio es ampliar el conocimiento de este eje S1P/SphK y su papel en la atrofia del músculo esquelético. Para ello, se utilizaron cultivos de células C2C12 murinas como mioblastos, precursores comprometidos; y miotubos, células totalmente diferenciadas; para imitar las condiciones de caquexia asociadas al cáncer mediante el uso de Dexametasona, un glucocorticoide sintético. Posteriormente, los cultivos celulares se trataron con un inhibidor de la histona deacetilasa (Trichostatin A) que se ha relacionado con mejoras en la prevención y regeneración de la atrofia muscular.

Se evaluó la variación de los niveles de expresión génica de SphK1, SphK2 (ambos), p21 (mioblastos) y Atrogin-1 (miotubos) mediante transcripción inversa y PCR en tiempo real. Los resultados mostraron en mioblastos una reducción de los valores de expresión; mientras que en los miotubos tratados con DEXA aumentaron significativamente, para después verse disminuidos tras el tratamiento con TSA, demostrando así el importante rol de las HDAC.

Palabras clave: *músculo esquelético, atrofia muscular, esfingolípidos, real-time PCR*

Autor/a: Alba María Candela Candela

Tutor/a académico/a: Dña. María Adelaida García Gimeno

Co-tutor/a: Dña. Elisabetta Meacci

Valencia, septiembre 2022

Agradecimientos

A Elisabetta, por ser un ejemplo y mi referente. Gracias por acogerme desde el primer momento y estar siempre dispuesta a que quiera volver, por demostrarme que puedo y conocerme mejor que yo misma en muchas ocasiones.

A Livia, por darle vida al laboratorio, cuidarme y motivarme a estar todos los días haciendo PCRs a las 10, sin importar en qué estado.

A Ada, por tu paciencia y tu profesionalidad. Gracias por tus consejos, tu atención y por la confianza depositada en mí.

A mis padres, por ser siempre mi mayor apoyo incondicional y hacer posible la vida que tengo. Especialmente a mamá, por estar siempre dispuesta a escucharme hablar de asignaturas que no entiendo ni yo por muy temprano o tarde que sea y no dejar que me rinda nunca.

A Carmen y Miguel, por estar hasta cuando yo no estoy.

A mis amigos Biotekes, porque sin vosotros creo que hubiese abandonado la carrera muchas veces. Por las sesiones de estudio, teóricas y prácticas, y por las menos responsables también.

A Firenze, porque allí también tuvo lugar el final de mi etapa en la carrera de biotecnología. Per essere la città più bella del mondo. Por lo efímero, las personas y los recuerdos que la hicieron hogar.

A Fio, por ser mi compañera de aventuras y siempre llevarme de vuelta a la *dolce vita.*

Sin vosotros, nada de esto habría sido posible. Gracias.

Index

Index of figures

Index of tables

List of abbreviations

ABC	ATP-binding cassette transporter
ActRIIB	Activin A receptor type IIB
Akt	Protein kinase B - Serine/threonine-specific protein kinases
AMPK	AMP-activated protein kinase
ATGs	Autophagy related genes
ATP	Adenosine Triphosphate
DEXA	Dexamethasone
DNA	Deoxyribonucleic Acid
eIF3f	Eukaryotic Translation Initiation Factor 3 Subunit F
ER	Endoplasmic reticulum
Fbxo40	F box protein 40
FoxO	forkhead-box protein O
GC	Glucocorticoid
GPCCRs	GTP-protein binding-coupled receptors
HAT	Histone Acetylase
HDAC	Histone Deacetylase
HDACI	Histone Deacetylase Inhibitor
IGF1	Immunoglobulin Factor 1
IKKβ	Inhibitor of Nuclear Factor Kappa B Kinase Subunit Beta
IL-1	Interleukin 1
IRS1	Insulin receptor substrate 1
LPP	Lipid phosphatase
Lys	Lysine
MAFbx	Muscle atrophy F-box
mTOR	mammalian target of rapamycin
MuRF1	Muscle RING finger 1
MyoD	Myogenic Differentiation Antigen
NF-κB	Nuclear factor kappa-light-chain-enhancer of activated B cells
P21	Cyclin-dependent kinase inhibitor 1
P53	tumour protein
PHB2	prohibitin 2
PI3K	phosphoinositol 3 kinase
S1P	Sphingosine 1-phosphate
S1PR	Sphingosine 1-phosphate receptors
SLs	Sphingolipids
SMAD	Suppressor of Mothers against Decapentaplegic
SphK1 y SphK2	Sphingosine kinases 1 and 2
Spns2	Spinster homolog 2
TNFα	Tumour Necrosis Factor α
TRAF2	tumour necrosis factor receptor-associated factor 2
TRAF6	Tumour Necrosis Factor Receptor Associated Factor 6
Trim32	Tripartite motif-containing protein 32
TSA	Trichostatin A
ZNF216	zinc finger 216

1. Introduction

1.1. Skeletal muscle atrophy and cachexia

Skeletal muscle tissue, the largest protein reservoir in the body and accounting for approximately 40% of total body weight, is a plastic organ that is maintained by multiple pathways regulating cell and protein turnover (Bonaldo & Sandri, 2013).

Muscle mass and muscle fibre size vary according to pathophysiological conditions. An increase occurs during postnatal development through a process of hypertrophy or enlargement of individual muscle fibres, and a similar process may be induced in adults in response to mechanical overload or hormonal stimulation. The regulation of muscle mass reflects protein turnover, which refers to the balance between protein synthesis and degradation within muscle fibres.

Muscle atrophy is defined as a decrease in the size of a tissue or organ due to cellular shrinkage; and cell size decreasing is caused by the loss of organelles, cytoplasm, and proteins; reflecting the hyperactivation of the cell's main degradation pathways (Schiaffino et al., 2013). Atrophy can appear in specific muscles with inactivity or denervation, systemically results from aging (sarcopenia) (Larsson et al., 2019), it is a physiological response to starvation, and it is also associated to many diseases as cancer (cachexia) (Argilés et al., 2019), diabetes or catabolic hormonal stimulation.

Excessive protein degradation in skeletal muscle can lead to cachexia, which is defined as a multifactorial syndrome characterised by an ongoing loss of skeletal muscle mass (with or without loss of fat mass) that cannot be fully reversed by conventional nutritional support and leads to progressive functional impairment. The pathophysiology is characterised by a negative protein and energy balance driven by a variable combination of reduced food intake and anormal metabolism (Fearson *et al.*, 2011). It occurs in the majority of cancer patients, although it can also be caused by other metabolic alterations in the patient even those resulting from chemotherapeutic treatment. Cachexia increases morbidity and mortality rates, reduces tolerance to medical treatments and affects negatively to patient quality of life. It can also affect adipose tissue, heart, intestine, kidney and liver as it is a multiorgan syndrome.

Nowadays, solutions to this condition are really limited, so several blood biomarkers for cancer cachectic patients have been suggested, although they are still on study phases. Some of them are tumour-derived compounds, inflammatory cytokines, acute-phase proteins and skeletal muscle and degradation markers (Argilés *et al.*, 2014).

As common proteolytic pathways are activated during diverse types of atrophy, understanding the set of processes by which muscle wasting happens will be crucial to target certain key components of these common mechanisms as it is likely to be beneficial in many diseases. Currently, the only validated treatment is exercise, which reduces various types of atrophy, but it is not a possible solution in cases of sarcopenia or cancer-associated cachexia (Lira *et al.*, 2015). Thus, there is an urgent medical need to develop drug therapies that will prevent or restore this muscle mass loss to improve patient quality of life and survival.

1.2. Molecular mechanisms of muscle wasting

These conditions are directly related to abnormalities in proteins synthesis and degradation and amino acid metabolism. Also, an increase in apoptosis and an impaired capacity for regeneration contributes to muscle wasting.

Protein synthesis is the process by which mRNA, is translated on ribosomes into amino acids and can be divided into three distinct phases: initiation, elongation and termination. Previously, translation is a key rate limiting process, controlled through the phosphorylation of initiation factors and protein kinases that are controlled by a variety of signalling pathways downstream of phosphatidylinositol 3-kinase (PI3K) (Bodine & Furlow, 2015).

The most important cell proteolytic systems involved in the wasting process are mediated by the activation of the ubiquitin-proteasome pathway and the autophagy-lysosome pathway. They involve a subset of atrophy-related genes that has been called 'atrogenes'. They are normally up- or down-regulated and have been identified in atrophying skeletal muscle, regardless of the catabolic condition (Bonaldo & Sandri, 2013).

1.2.1. Ubiquitin-dependent proteasome pathway

Ubiquitin-proteasome system is required to remove sarcomeric proteins in response to changes in muscle activity. Different classes of enzymes are involved in protein ubiquitination: E1 works as the ubiquitin activating, E2 as the ubiquitin conjugating and E3, which is the ubiquitin ligase, binds the protein substrate and catalyses the movement of the ubiquitin from E2 to the substrate. This is the rate-limiting step of the process and affects the subsequent proteasome-dependent degradation (Sandri, 2016).

A decrease in muscle mass is associated with increased conjugation of ubiquitin to muscle proteins; increased proteasomal ATP-dependent activity; increased protein breakdown that can be efficiently blocked by proteasome inhibitors; and upregulation of transcripts encoding ubiquitin, some ubiquitin-conjugating enzymes (E2), a few ubiquitin-protein ligases (E3) and several proteasome subunits.

Among the known E3 family, there are a few both muscle-specific and up-regulated during muscle protein depletion so they were considered the master genes in muscle atrophy. Atrogin-1/MAFbx and MuRF1 were the first identified and it has been shown that their expression increase expression increase rapidly upon a variety of stressors, such as GC and pro-inflammatory cytokines, cancer cachexia and other pathological states.

In muscle homeostasis, once the substrate is polyubiquitylated, it is docked to the proteasome for degradation. The components of the ubiquitination involved in muscle wasting are depicted in Fig. 1, where E3 ubiquitin ligases are depicted in green, with arrows pointing to their substrates. Note that ubiquitin ligases can have different cellular localizations and can shuttle into the nucleus.

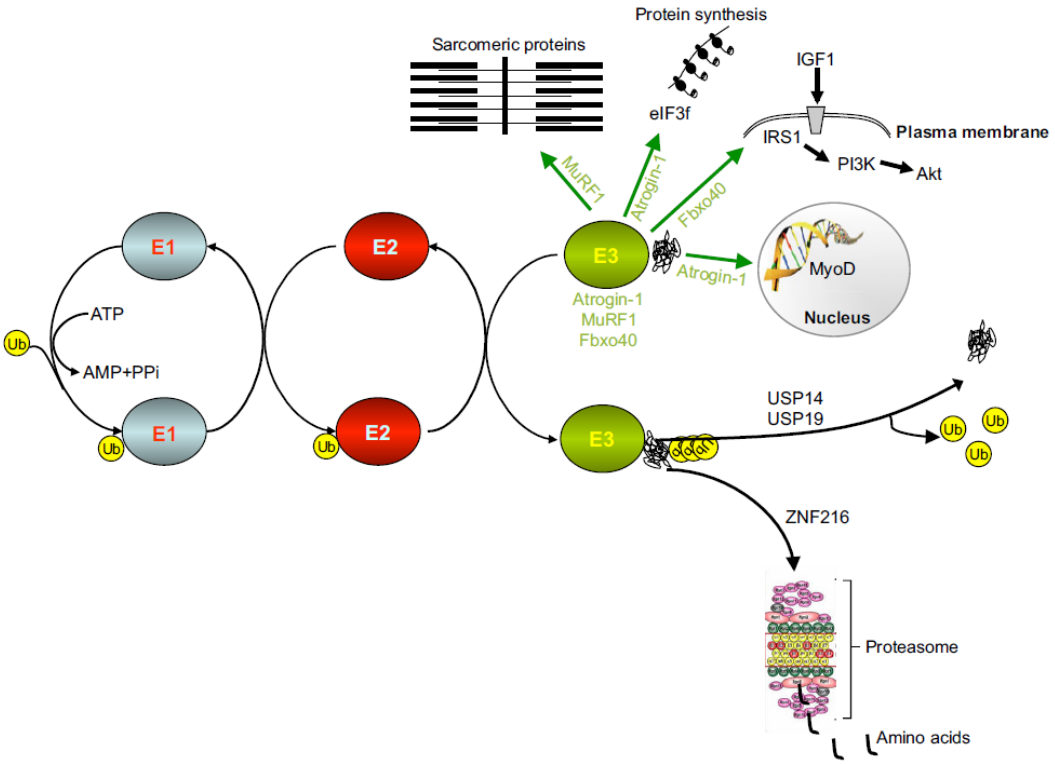

Figure 1. **Ubiquitin-proteasome degradation pathway**. Mechanism of activation, main enzymes (E1, E2 and E3) and further processes promoted by E3 ligases linked to atrophy (Atrogin-1, MuRF-1 and Fbxo40). ZNF216 mediates proteasome action and USPs develop de-ubiquitination process.

Atrogin-1 promotes degradation of the MyoD, a key muscle transcription factor, and of eIF3f, an important activator of protein synthesis. MuRF1 was reported to interact and control the half-life of several sarcomeric proteins, including troponin I, myosin heavy chains, actin, myosin binding protein C and myosin light chains 1 and 2. The transcription factor myogenin, an essential regulator of muscle development, is required for the maximal activation of these two genes.

Presumably, there are other E3s activated during atrophy like Trim32, crucial for the degradation of the filaments, or TRAF6, that mediates the conjugation of Lys63-linked polyubiquitin chains to its target proteins and it is required for optimal activation of FoxO3, NF-κB and AMPK, which act as regulators of Atrogin-1 and MuRF1 expression. In skeletal muscle, it was found that Fbxo40 regulates degradation of IRS1, an essential factor for IGF1/insulin signalling, and ZNF216 is an important player in the recognition and delivery to the proteasome of ubiquitylated proteins during muscle atrophy as it is up regulated by FoxO transcription factors. Still, there is still much research on this field to known between ubiquitylation and de-ubiquitylation process and its contribution to muscle atrophy. The largest class of de-ubiquitylating enzymes are the ubiquitin-specific processing proteases (USPs) and only USP14 and USP19 have been found to be upregulated in atrophying muscles (Bonaldo & Sandri, 2013).

1.2.2. Autophagy-lysosome pathway

It is an evolutionarily conserved catabolic process through which damaged organelles and macromolecules are degraded and recycled within the cell. It occurs in response to various stimuli such as cellular stress, nutrient deprivation, amino acid starvation and cytokines. In mammals, three different mechanisms have been described: macroautophagy, chaperone-mediated autophagy and microautophagy. Most data on autophagic process in muscle are focused just on macroautophagy, hereafter named autophagy (Bonaldo & Sandri, 2013).

Skeletal muscle is one of the tissues with the highest rates of vesicle formation. This process involves a number of conserved autophagy-related genes (ATGs), transcriptionally regulated, and proceeds through the following steps: 1) induction, 2) double-membrane commitment to form the phagophore or isolation membrane, 3) membrane elongation to form autophagosome and sequestration of cellular components; 4) autophagosome-lysosome fusion, 5) degradation of sequestered components and recycling of amino acids, lipids and glucose; 6) lysosomal rejuvenation and biogenesis (Sandri, 2016).

Autophagy is activated in catabolic conditions, under FoxO regulation, so a regulatory complex induces membrane elongation and autophagosome formation.

Autophagy involvement in muscle protein breakdown was not recognised for a long time. It is now known that also plays a crucial role, but further research is needed. Although it was initially considered a non-selective degradation pathway, it is becoming evident the presence of more selective forms for specific organelles, as mitophagy for damaged and dysfunctional mitochondria (Bonaldo & Sandri, 2013).

1.3. Signalling pathways regulating muscle atrophy

Pathways that control protein breakdown in muscles are related to cell growth, nutrients homeostasis, ATP production and inflammatory cytokines. Transcription factors are the endpoint of these pathways, so all of them regulate the expression of atrogenes in some way and they all converge on the Akt-FoxO signalling axis.

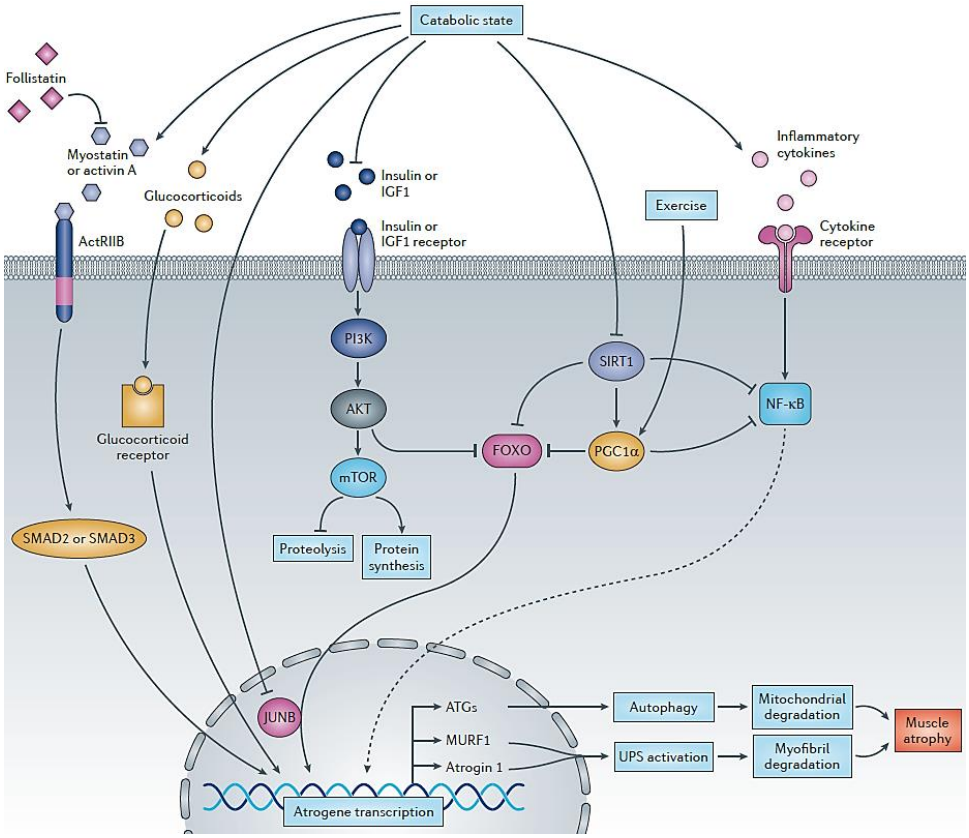

Figure 2. **Signalling pathways leading to atrogene transcription, thus to muscle atrophy**. Triggering routes inducing protein degradation by ubiquitin-proteasome and autophagy-lysosome pathways involve activation of atrogene transcription factors by Insulin (IGF1)-Akt-FoxO, nuclear factor NF-κB, SMAD2 and SMAD3, or glucocorticoids, among others.

1.3.1. IGF1-Akt-FoxO signalling

Insulin-like growth factor 1 (IGF1) is a circulating growth factor produced by many tissues, including skeletal muscle. Diverse studies have shown that its overexpression sustains muscle growth and regeneration, and it can also supress protein breakdown. Further understanding of this pathway was achieved from studies of Akt, also known as Protein kinase B, which is a set of three serine/threonine-specific protein kinases hat play key roles in multiple cellular processes such as glucose metabolism, apoptosis, cell proliferation, transcription, and cell migration.

Akt controls both protein synthesis, through mTOR kinase, and protein degradation, via transcription factors of the FoxO family. Among this group, FoxO1, FoxO3 and FoxO4 are present in skeletal muscle and induce components of ubiquitin-proteasome system and autophagy.

There is a crosstalk between Akt and FoxO: Akt phosphorylates FoxO proteins, promoting their export from the nucleus to the cytoplasm with further activation of Atrogin-1 and MuRF1 and thus suppression of protein breakdown. The up-regulation of Atrogin-1, MuRF1 and several autophagy-related genes is normally blocked by Akt through negative regulation of FoxO transcription factors, suppressing protein synthesis. Remarkably, FoxO activity is regulated by several different post-translational modifications, including phosphorylation, acetylation, and mono- and polyubiquitylation. Recent evidence suggest that acetylation negatively regulates

FoxO3 activity while has no effect on FoxO1. Also, there was found a connection between AMPK and FoxO3, where the latter is activated via AMPK phosphorylation of several Akt-independent sites, stimulating the expression of Atrogin-1 and MuRF1 in stress conditions. AMPK has been also related to induction of some autophagy-related genes.

PGC1α is a critical cofactor for mitochondrial biogenesis that has been found to interact with FoxO. High levels of PGC1α and its homolog PGC1β spare muscle mass during catabolic conditions by the inhibition of autophagy-lysosome and ubiquitin-proteasome degradation pathways. They also reduce protein breakdown by inhibiting transcriptional activity of FoxO3 and NF-κB, but they do not affect protein synthesis (Bonaldo & Sandri, 2013).

1.3.2. Inflammatory cytokines and NF- κB signalling

Nuclear Factor-kappa B (NF-κB) transcription factors are expressed in skeletal muscle and activated by pro-inflammatory and pro-cachectic cytokines, such as interleukin-1 (IL-1) or tumour necrosis factor (TNFα), being the latter especially important.

In the inactive state, NF-κB is sequestered in the cytoplasm by binding of a family of inhibitory proteins called IκB. In response to TNFα, the IκB kinase (IKKβ) is activated and phosphorylates IκB, resulting its ubiquitination and proteasomal degradation. This leads to nuclear translocation of NF-κB and activation of NF-κB-mediated gene transcription.

One of the effects of TNFα and pro-inflammatory cytokines is to induce insulin resistance and suppression of the IGF1–Akt pathway. Also, TNFα treatment causes up-regulation of MuRF1 and Atrogin1/MAFbx and myogenin.

TNF-like weak inducer of apoptosis (TWEAK) was found to induce muscle atrophy by binding to fibroblast growth factor-inducible (Fn14), which allows NF-κB activation and MuRF1 expression when upregulated.

The ubiquitin ligase TRAF6 is another important in NF-κB signalling and it is required for Fn14 upregulation, and also for the activation of FoxO3 and AMPK, and for the induction of ubiquitin-proteasome and autophagy-lysosome pathways (Schiaffino *et al.*, 2013).

1.3.3. Myostatin and SMAD2 and SMAD3

Myostatin, the major autocrine inhibitor of muscle growth, is a member of the TGFβ family. It is expressed and secreted predominantly by skeletal muscle and binds to the activin A receptor type IIB (ActRIIB) inducing fibre atrophy through activation of the transcription factors SMAD2 and SMAD3. It is known that glucocorticoids, FoxO1, NF-κB, and SMAD2 and SMAD3 can all enhance myostatin expression.

Myostatin was reported to up-regulate essential atrophy-related ubiquitin ligases and this regulation was found to be FoxO dependent. In fact, myostatin treatment blocks the IGF1-Akt pathway and activates FoxO1, allowing increased expression of atrogin-1. This crosstalk between the two pathways does not require NFκB, whose inhibition does not prevent upregulation of atrogin-1 (Cohen *et al.*, 2015; Schiaffino *et al.*, 2013).

1.4. Glucocorticoid-induced muscle atrophy

Glucocorticoids (GC) are a group of steroid hormones produced by the adrenal cortex in response to environmental or biological stress. They are involved in a variety of biological processes including metabolism, cardiac output, inflammation, and immunity.

In many pathological conditions, such as sepsis, cachexia or starvation, GCs levels are increased. They decrease the rate of protein synthesis and increasing protein breakdown, thus leading to muscle wasting. Glucocorticoids are known to have catabolic effects on skeletal muscle, either as an endocrine hormone released in response to stress or as a drug.

Synthetic glucocorticoids are used to treat a variety of inflammatory diseases in humans and can induce muscle atrophy in both the acute and chronic phase of treatment. Moderate to high doses produce the synthesis of muscle proteins significantly, and at low doses they attenuate the ability of branched chain amino acids and insulin to activate protein translation (Bodine & Furlow, 2015).

Several studies reported that GC administration to myocyte cultures results in activation of common intracellular signalling pathways that eventually generate a hypercatabolic drive comparable to that occurring in cachexia. Also, GCs are extensively used as a component of chemotherapy, contributing to cancer and chemotherapy-induced cachexia. Therefore, GCs are widely used in medical research, to actually fight some inflammation-related diseases, but also to induce protein breakdown and mimic skeletal muscle atrophy conditions. For these reasons, GCs have been used to expose C2C12 cells inducing muscle atrophy in this study.

In particular, dexamethasone (DEXA) has been chosen in this study as it is a synthetic GC as it has been previously used and its mechanisms are well-known. Like other GCs, it has been reported to act either by interference with the insulin/IGF-I signalling pathway (non-genomic action) or by transcriptional stimulation of Atrogenes, via several transcriptional factors, in particular FoxO activation and mTOR inhibition. They also stimulate the ubiquitin-proteasome and autophagy-lysosome pathways (Schakman *et al.*, 2013).

1.5. Sphingolipids

Sphingolipids (SLs) are a large group of metabolites that represent one of the major classes of eukaryotic lipids. They can be found in the cellular membrane and are emerging as biologically active factors, which seem to have an important role in biological functions and its regulation (Meacci *et al.*, 2008).

This group is composed of sphingosine backbone linked to one hydrophobic acyl chain and a phosphate head group ester. The main bioactive sphingolipids are ceramide, sphingosine and sphingosine 1-phosphate (S1P). The latter appears to be especially important because of its function as a survival and trophic factor, which increases cell proliferation and differentiation, and inhibits apoptosis. The attention of this study will be focused on S1P.

1.5.1. Metabolism

Cellular synthesis and degradation of S1P involves multiple enzymes, some expressed as various isoforms with different biochemical properties and cellular locations, indicating a highly complex metabolism. Some of the major enzymes these processes are Ceramidase, which catalyses the hydrolysis of Ceramide into Sphingosine and a free fatty acid; sphingosine kinases (SphK), which catalyses the ATP-dependent phosphorylation of Sphingosine; S1P phosphatases, with the opposite effect towards degradation; and S1P lyase, a degrading enzyme by cleavage.

As shown in Fig. 3, 1P cannot be produced through by *de novo* synthesis, but it can be obtained by the series of enzymatic actions on different metabolites (Pierucci *et al.*, 2018; Olivera *et el.*, 2013).

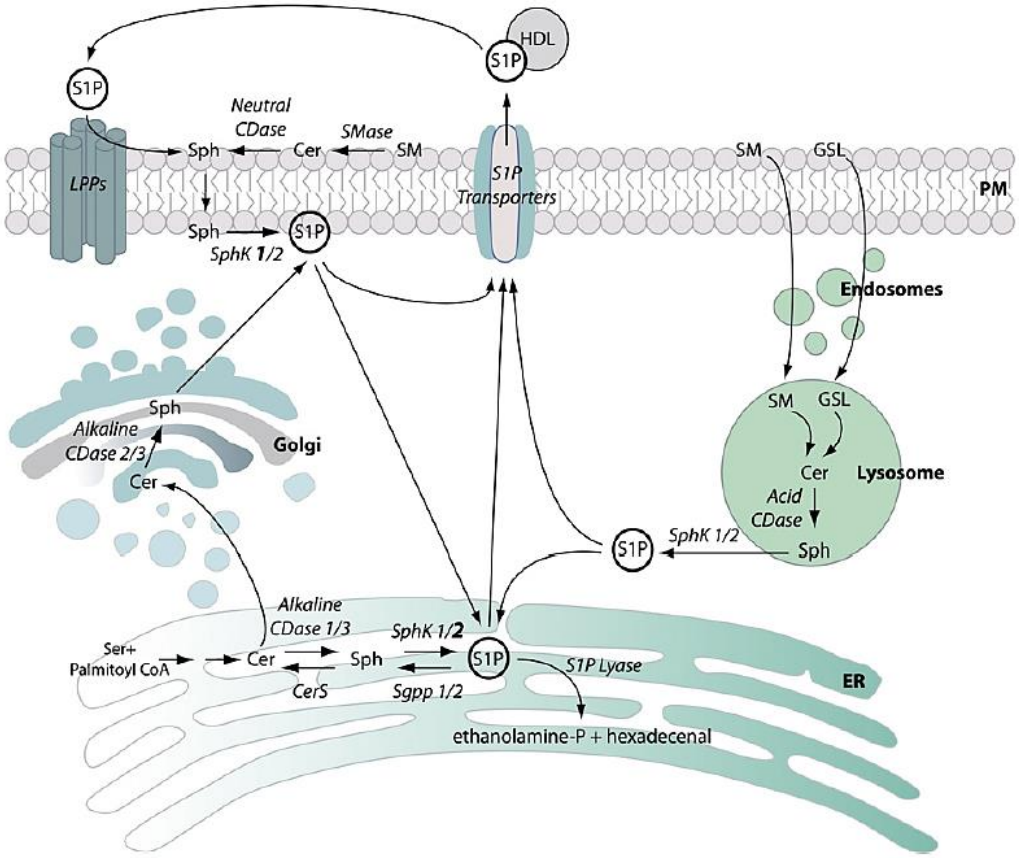

Figure 3. **Sphingosine 1-phosphate (S1P) formation, transport and degradation sphingolipid metabolism**. SphK1 and SphK2 produce S1P synthesis from sphingosine, obtained from degradation of Ceramide, in different subcellular locations: cytoplasm for SphK1, while nucleus and mitochondria for SphK2. S1P needs transporters to translocate out of the cell for autocrine/paracrine signalling. Degradation can be performed either inside or outside the cell by phosphatase or lyase action.

S1P synthesis by Sphingosine Kinases (SphK) can occur after the degradation of Ceramide, which takes place in the ER and in the Golgi after *de novo* synthesis, or in the lysosomes and at the plasma membrane, during catabolism of Sphingomyelin and glycosphingolipids. Ceramide degradation to Sphingosine is performed by any of five Ceramidases: acid, neutral, and three alkaline ceramidases.

Two isoforms of SphK have been described, SphK1 and SphK2, each of which has distinct catalytic activities, intracellular locations, and tissue distributions, suggesting unique functions. SphK1 is largely cytoplasmic and can acutely associate with plasma membranes, while SphK2 is present in the cytoplasm but is predominately in specific subcellular compartments, as the nucleus or the mitochondria.

Degradation of sphingosine 1-phosphate can be performed by S1P lyase, generating phosphorethanolamine and hexadecenal, or by S1P phosphatases, ending up in Sph again. As for extracellular degradation, S1P can be dephosphorylated by a group of lipid phosphatases (LPP), liberating sphingosine, which can be re-phosphorylated back to S1P (Meacci & Garcia, 2019).

1.5.2. S1P/S1PR Signalling

As it is largely produced within the cell, S1P may move rapidly between cell compartments acting as an intracellular mediator; as well as it can be secreted outside the cell. It is relatively hydrophilic due to its charged polar head group, it is unable to diffuse over the membrane, so it requires transporters to exit the cell: ATP-binding cassette (ABC) transporters and by spinster homolog 2 (Spns2) transporter. Once outside the cell it can act as an autocrine or paracrine signal by binding to its five specific heterotrimeric GTP-binding protein-coupled receptors (GPCCRs), hereinafter referred to as S1P receptors (S1PR). These processes are further illustrated in Fig. 4.

S1PRs mediate diverse cellular functions through differential coupling to G-proteins, involved in multiple downstream signalling pathways. Thus, it indicates that S1P action can be highly modulated and mediated by many signalling pathways. These receptors have different expression within tissues and also between normal and malignant human conditions, mainly located at plasma membrane. It is known that S1PR1, S1PR2 and S1PR3 are expressed in skeletal muscle tissue (Meacci & Garcia, 2019). These receptors mediate binding of S1P to its receptor plays a key role in cytokine production and in anti-apoptotic response (Cordeiro *et al.*, 2019).

S1PR activation modulates extracellular signal–regulated kinases, such as phosphoinositide 3-kinases (PI3K) and, in turn, multiple signalling pathways.

S1P can activate different intracellular targets and plays a critical role in differentiation, epidermal homeostasis, inflammation and tumour immune response. Some of the targets have been identified in cytoplasm, mitochondria and nucleus: prohibitin 2 (PHB2), a highly conserved protein that regulates mitochondrial assembly and functions; or tumour necrosis factor receptor-associated factor 2 (TRAF-2), a key adaptor molecule in tumour necrosis factor receptor signalling complex, which has an E3 ubiquitin ligase activity and is a key component of the nuclear factor-κappa B (NF-κB) pathway, crucially involved in inflammatory gene regulation. Plus, recent studies suggest its interaction with histone deacetylases (HDACs) or human telomerase, among others, which indicates a lot to further research in this field.

Related to its location, S1P formed by SphK1 seems to translocate after activation to the plasma membrane, mediating cell proliferation and survival. It has been observed that enhanced SphK1 is correlated with neoplastic transformation and tumorigenesis and pharmacological inhibition of the enzyme attenuates tumour growth. Furthermore, it has been found that SphK2 can promote cell cycle arrest and apoptosis, an opposite effect compared to SphK1. In addition, when located

into the nucleus, SphK2 mediates DNA synthesis inhibition and HDAC regulation, whereas when it is present in the mitochondria, promotes programmed cell death by collaborating with pro-apoptotic proteins.

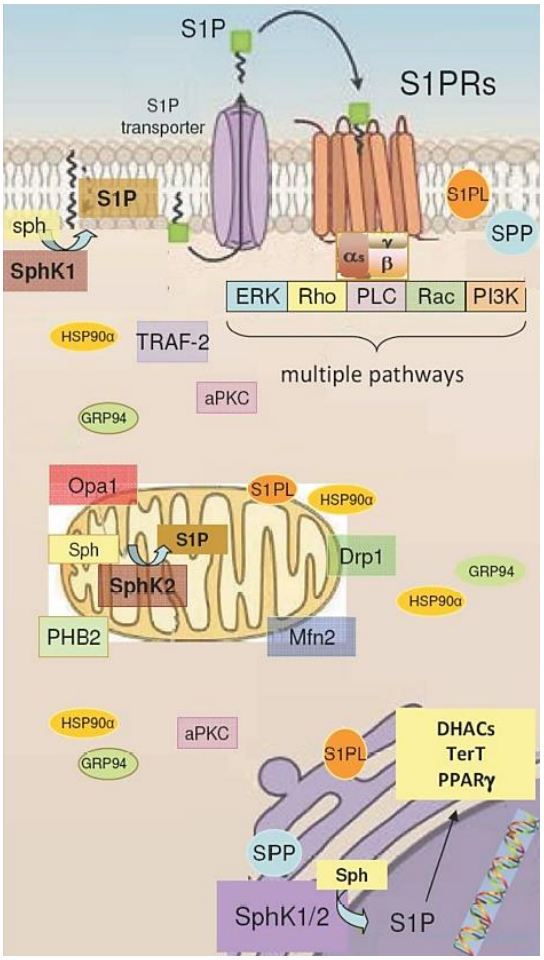

Figure 4. Sphingosine 1-phosphate (S1P) and SphK1 and SphK2 signalling pathways and components in different subcellular locations.

Some studies reported that S1P can associate with histone H3 and control the binding of acetyl groups to lysine residues within histone tails through HDAC1/HDAC2 regulation. In particular, nuclear SphK2/phospho-SphK2 and S1P co-immunoprecipitated with HDAC1/2 leading to increased histone acetylation at several lysine residues of histone H3. Therefore, HDACs are direct intracellular targets of SphK2/S1P axis and SphK2 is a part of repressor complex and support the involvement of S1P in the epigenetic regulation of gene expression. SphK2 and the active phospho-SphK2 associate with HDAC1/2 as part of these two co-repressor complexes. The formation of these complexes at the promoter of genes encoding pro-inflammatory cytokines, is crucial for the ability of SphK2 to modulate inflammation and tissue injury (Meacci & Garcia, 2019).

1.6. Histone Deacetylases (HDACs)

A step before mRNA translation into proteins, DNA transcription is key. Regulation of this process occurs within the nucleus of eukaryotic cells and requires an extreme compaction of DNA, which is possible through its association to a protein group called histones. DNA is negatively charged due to phosphodiester linkages throughout its structure, while the histone proteins are positively charged due to the abundant presence of lysine residues. In this way, electrostatic attraction forces between DNA and the histones hold them together and form the structure known as chromatin. Furthermore, DNA accessibility is also regulated depending on some modifications of chromatin structure. It involves the recognition of covalent modifications in the histone N-terminus.

Epigenetics refers to all molecular processes and mechanisms that affect gene regulation and expression, of which DNA methylation and post-translational modification of DNA-associated histones are the most common forms, including acetylation, methylation, phosphorylation and ubiquitinoylation (Fernández, 2014).

1.6.1. Histone acetylation and deacetylation

This study involves reversible acetylation and transcription regulation as high levels of this modification have been linked to gene activation, whereas histone deacetylation corresponds with gene repression.

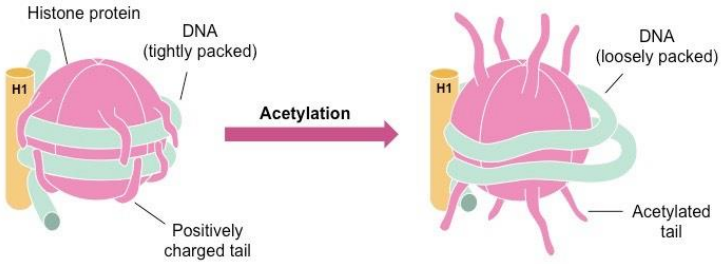

Figure 5. **Histone acetylation process to promote gene transcription**. Post-translational modifications allow the sight release in chromatin compaction that promote transcriptional factors to start the process.

Histone acetylation is carried out by a class of enzymes known as histone acetyltransferases (HATs), which catalyse the transfer of an acetyl group from acetyl-CoA to the lysine on the N-terminal tails of histones. Histone acetyltransferase complexes are involved in such diverse processes as transcription activation, gene silencing, DNA repair and cell-cycle progression.

In the regions where the histone tails associated with DNA are acetylated, chromatin is in a low state of condensation, so it allows the molecular machinery for gene transcription to enter (Fig. 5). This happens because added neutral acetyl groups modify and reduce the intrinsic positive charge or the multiple lysine residues, decreasing their affinity and relaxing the histone-DNA binding. The reverse process is performed by enzymes called histone deacetylases (DHACs), that are responsible for the elimination of acetyl groups present in the lysine residues, which makes the chromatin structure much more compact. Therefore, in actively transcribed regions of chromatin, histones tend to be hyperacetylated, whereas in transcriptionally silent regions

histones are hypoacetylated (Carrozza *et al.*, 2003). Moreover, HDACs can also regulate gene expression by binding directly to transcription factors or nuclear receptors.

It has been demonstrated that altered activity of histone acetylation/deacetylation processes play a crucial role in the progression of various diseases, such as cancer. Abnormal levels of acetylation may be caused not only by decreased HAT activity (due to mutations or chromosomal translocations), but also by increased or altered HDAC activity.

The latter is the most studied as it has been linked to tumour progression, not because of altered levels of expression of HDAC, which has also been associated with cancer, but by its action at the wrong sites. Therefore, it produces translocation of large sections of genes that, when transcribed and translated, result in fusion proteins that recruit HDAC to form gene-repressing complexes so that they bind to the promoters of genes that regulate myeloid cell differentiation and proliferation, leading to tumour development (Fernández, 2014).

It is intriguing how HDACs modify gene expression in the skeletal muscle tissue in response to humoral factors, and that, in turn, several HDACs modulate the expression of soluble factors, ultimately affecting their levels in the circulation (Renzini *et al.*, 2022).

1.6.2. HDAC inhibitors: Trichostatin A (TSA)

A critical role of specific HDAC proteins emerged in the regulation of skeletal muscle atrophy, as some kinds have been linked to activating signalling pathways, inducing MuRF1 and Atrogin1/MAFbx expression (Beharry & Judge, 2015).

Further, HDACs have also a key role in acetylation processes of non-histonic proteins. As an example, they deacetylate the p53 tumour suppressor factor, which altered activity leads to uncontrolled cell division and resistance to pro-apoptotic signals.

Given the importance of these processes and main enzymes, this and other studies have focused on testing molecules that can inhibit HDAC activities, restoring normal expression of genes and proteins. In this way, histone deacetylase inhibitors (HDACIs) are on the spotlight as promising treatments (Hagiwara *et al.*, 2011).

The best-known compounds with these characteristics are hydroxamic acids, of which this work will focus on Trichostatin A. Generally, hydroxamic acids act by chelating Zn^{2+} atoms directly on the active site of HDACs (Fernández,2014), inhibiting its action. TSA, which structure is shown in Fig. 6, is an antifungal antibiotic and one of the most powerful HDACI versus class I and II of HDACs.

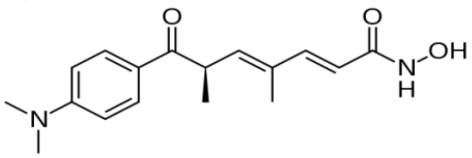

Figure 6. Formula and structure of Trichostatin A.

Previous studies suggest that, in C2C12 cells, TSA may have some effects preventing some types of atrophy with evidence on the increased levels of MuRF1 being reversed (Dupré-Aucouturier *et*

al., 2015) or the on the recruitment and fusion of myoblasts into preformed myotubes. It was demonstrated that when TSA is transiently applied to C2C12 myoblasts and differentiation is then induces, enhanced muscle formation is exhibit. It was then suggested that TSA promotes the expression of genes that work in the proliferation stage of muscle formation and supresses those working in the differentiation stage (Hagiwara *et al.*, 2011; Renzini *et al.*, 2022).

A family of cyclin-dependent kinases (cdk) are key regulators of cell cycle progression involved in cell proliferation. The cdk inhibitors bind to the cdk to function as negative regulators of cell proliferation. One of these molecules is p21, which can also act as a direct inhibitor of DNA polymerase. It was seen that upregulation and sustained expression of p21 are important features of terminal cell cycle arrest during myocyte differentiation (Guo *et al,* 1995)

2. Objectives

- Investigate the role of S1P/S1PR axis in skeletal muscle atrophy
- Study the role of Sphk1 and Sphk2 in the induction of myoblast differentiation by Trichostatin A
- In a model of atrophy induced to C2C12 cells through Dexamethasone, characterise the variations and improvements in SphK/S1P axis when they are treated with Trichostatin A

3. Materials and methods

3.1. Materials

Dulbecco's Modified Eagle's Medium (DMEM), fetal bovine serum (FBS, penicillin/streptomycin, horse serum (HS), TRI Reagent solution, Phosphate Buffered Saline (PBS), trypsin 1X, protease inhibitor cocktail and DNaseI were purchased from Sigma Aldrich (Milan, Italy); C2C12 myogenic cells, human primary skeletal muscle cells, were obtained from American Type Culture Collection (ATCC, Manassa, VA, USA); dexamethasone (DEXA) was from Tocris (Bristol, UK); high capacity cDNA-Reverse-Transcription kit and Syber Green reagent, Nanodrop Spectrophotometer and PCR Master Mix were from Life Technologies (Thermo Fisher Scientific, Carlsbad, CA, USA); MIC qPCR cycler (Diatech Pharmacogenetics, Jesi, AN, Italy).

3.2. Methods

3.2.1. Cell cultures

Murine C2C12 skeletal myoblasts were routinely grown in Dulbecco's Modified Eagle's Medium (DMEM, Sigma) supplemented with 10% fetal bovine serum (FBS, Sigma), and a solution of glutamine and a mix of 1% antibiotics, including penicillin and streptomycin. They were cultured in P60 (60 mm diameter) Petri plates and placed in the incubator at 37ºC in humidified atmosphere containing 5% of CO_2 and 21% of O_2.

At the beginning of the study, cell cultures were constantly divided into two fresh plates to amplify the number of cells that will be under experimentation. After 36-48 hours, cells usually reach a high enough confluence (70-80%) to be conduct the following procedure:

1) Add 2 mL of phosphate buffered saline (PBS), a balanced salt solution used when further cell culture applications must be performed. In these conditions, it was used specifically to wash FBS and prevent it from blocking the action of Trypsin.
2) Add 0,5 mL of Trypsin for 3-5 minutes to detach cells from the well bottom.
3) To dilute the Trypsin and count, collect the cells in 1-2 mL of DMEM (10% FBS), from where 7µL will be introduced into each of the partitions between the microscope slide and the cover glass.

At this moment, a cell counting step must be carried out to determine the number of cells per unit of volume (mm^3). For that use, it was decided to use the Bürker chamber, which is composed by two identical partitions, each of which has 9 large squares (1 mm^2 each) divided by double lines (0,05 mm apart) into 16 group squares. These double lines form small 0,0025 mm^2 squares and the chamber depth is 0,1 mm.

The cells were counted in five large squares, highlighted in yellow in Fig. 7, in both partitions so a value for the average among the total ten squares can be obtained. The area of the square is 1 mm x 1 mm = 1 mm^2. The depth of each square is 0.1 mm. Hence, the final volume of each square at that depth is 1 mm^3. The total number of cells is calculated by the following formula:

Where *dilution factor* refers to the total volume added to the cellular content, including the 1-2 mL of DMEM and the previous 0,5 mL of Trypsin.

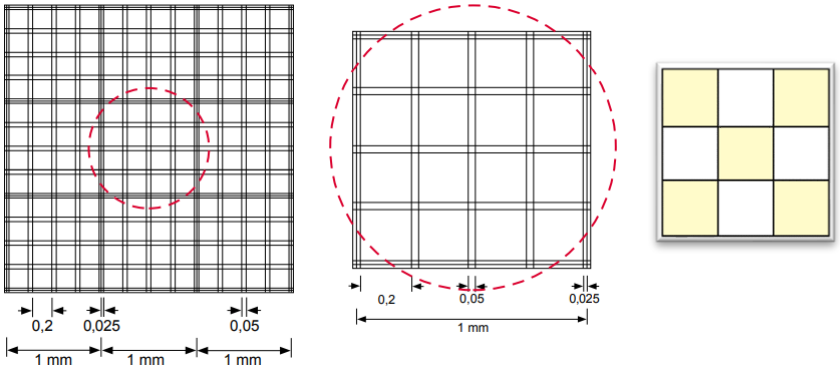

$$nº\ cells = average * 10^4 * dilution\ factor$$

Figure 7. Bürker chamber composition and calculus for total cell number.

For myoblasts experiments, cells were seeded in 6-well plates corresponding to P35 (35 mm diameter) at the concentration of 1,5 x 10^5 cells/well and treatments were applied when they reached 100% confluence.

In myotubes experiments, differentiation must be induced so cells were seeded the same way as previously explained until cells reached maximum confluence (after 72 hours). Then, the medium was replaced to differentiation medium (DM), composed of DMEM containing antibiotics, glutamine and 2% horse serum (HS). The medium was changed every 48 hours, occasionally washing with PBS to avoid contamination. Complete cell differentiation can be observed around 10 days after that (14-16).

3.2.2. Treatments

C2C12 myoblasts and myotubes cells will be exposed to different combinations of these treatments:

- Histone deacetylase inhibitor called Trichostatin A (TSA) at 150nM concentration
- Synthetic glucocorticoid called Dexamethasone (DEXA) at 100 µM concentration

TSA in myoblasts will be evaluated as it is supposed to induce cell differentiation into myotubes. In myotubes, TSA will be also performed to understand its effects in differentiated muscle cells, but cells will be also treated with DEXA to induce cancer-associated cachexia. Then, they will be exposed to TSA treatment to investigate the mechanisms how this inhibitor is able to approach normal gene expression, improving skeletal muscle atrophy condition.

3.2.3. Experiments

Three experiments have been developed as detailed in Fig. 8, two of them in myoblast cells (MB) and one in myotubes (MT).

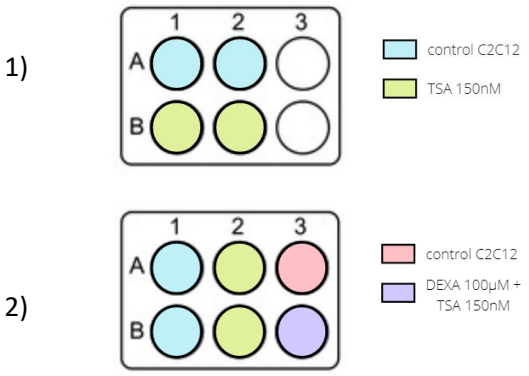

Figure 8. **Experiments performed in myoblasts (1) and myotubes (2).** Experiment 1 in myoblasts is represented in the 1 column, being blue for control and green for TSA 150nM; as well as experiment 2 is represented in column 2. Cells in experiment 1 were exposed to TSA for 24 hours, while experiment 2 lasted 48 hours.

Myoblasts

The first myoblast experiment (MB Exp 1) intended to notice the effect of Trichostatin A consisted in a simple comparison of one well used as a control of healthy C2C12 vs. the other, TSA-treated at 150nM and incubated during 24 hours at 37ºC.

MB Exp 2 presented the same conditions, but the duration of the exposure inside the incubator was 48 hours long to check if time of exposure had significant changes on effect.

Myotubes

Experiment on myotubes number 1 (MT Exp 1) mixed both DEXA and TSA treatments so it could reveal some information about treating atrophy-induced skeletal muscle cells with TSA and the variations observed. It was performed in a 6-well plate as following described: two wells of control cultures, one well for DEXA-treated cells at 100µM concentration, two wells for TSA-treated cells at 150nM and one last well for the combination of DEXA 100µM and TSA at 150nM.

2.4. RNA extraction and transcription

The process of extraction used to obtain total amount of RNA was performed using TRI Reagent solution (Sigma) protocol. TRI Reagent is a mixture of guanidine thiocyanate and phenol in a monophase solution normally used for the isolation of DNA, RNA and protein from biological samples of human, animal, plant, yeast, bacteria and virus.

Once cell treatments were completed, samples were homogenized using 1 mL of the solution per 50-100 mg of cells as the volume of the tissue must not exceed 10% of the volume of TRI Reagent in order to work with minimal shearing of the DNA. After this step, if needed, samples can be stored at -70ºC for up to 1 month.

The aim is to finally obtain the RNA fraction, so the first step was to centrifugate at 12,000 x g for 10 minutes at 4ºC to remove the insoluble material (extracellular membranes, polysaccharides, and high molecular mass DNA). The supernatant must contain just RNA and protein, so it was transferred to a fresh tube.

Next step was phase separation by adding 0,2 mL of chloroform per mL of TRI Reagent used and shaking vigorously for 15 seconds. It stood 2-15 minutes at room temperature to ensure complete dissociation of nucleoprotein complexes and then, the resulting mixture was centrifugated again at 12,000 x g for 15 minutes at 4ºC, so it was separated into 3 phases: a red organic phase (containing protein), an interphase (containing DNA), and a colourless upper aqueous phase (containing RNA).

RNA extraction protocol is reported bellow:

1. Transfer the aqueous phase to a fresh tube and add 0,5 mL of 2-propanol per mL of TRI Reagent and mix
2. Allow the sample to stand for 5-10 minutes at room temperature
3. Centrifuge at 12,000 x g for 15 minutes at 4ºC
4. Remove the supernatant
5. Wash the RNA pellet by adding a minimum of 1 mL of 75% ethanol per mL of TRI Reagent used
6. Mix (without vortex) the sample and then centrifuge at 7,500 x g for 5 minutes at 4ºC
7. Briefly dry the RNA pellet for 5-10 minutes by air-drying. (Do not let dry completely, as this will greatly decrease its solubility)
8. Add 12-15 µL of water and mix by repeated pipetting

Quantity and quality of the RNA isolated in the samples were measured using a wavelength of 260 and 280 nm via Nanodrop (Thermo Scientific). Final preparation ought to be free of DNA and proteins, so it should present a A260 to A280 ratio ≥ 1,7.

Next step was to synthetise first-strand cDNA parting from the RNA obtained. For that purpose, cDNA Reverse Transcription kit (Life Technologies, ThermoFisher) was used via two-steps reaction starting from the volume corresponding to 500 ng RNA of each sample.

First step consists in removing DNA from the RNA preparation prior to the sensitive following amplification. Thus, DNase I (Sigma) is key for this reaction as it is an endonuclease isolated from bovine pancreas that digests double and single stranded DNA into oligo and mononucleotides. Reagents in this reaction are:

- 1 µL of 10X Reaction Buffer
- Double Distilled Water (ddH_2O) + RNA (500 ng) adding up to 10 µL
- 1 µL of DNase I

After 15 minutes at room temperature, add 1 µL of Stop Solution and heat at 70ºC for 10 minutes to denature both the DNase I and the RNA. In the meantime, a Master Mix for the last step of the RT-PCR reaction must be prepared as detailed in Table 1:

Master Mix composition	
volume (µL)	reactive
3,2	ddH_2O
2	10X RT Buffer
2	10X Random Primers
0,8	dNTP mix
1	RNA inhibitor

Table 1. Master mix composition for one-sample reaction.

The quantities must be multiplied by the number of samples to amplify (+1 to ensure accuracy). This calculation corresponds to 9 µL for each sample. It was not until the last moment that the addition of RT enzyme happened, trying to avoid denaturation. Samples were finally incubated for 10 min at 25ºC, 120 min at 37ºC and 5 min at 85ºC; and stored at -20ºC.

2.5. Amplification and quantification of RNA

Quantitative real-time polymerase chain reaction (qPCR) is the technique of continuous monitoring of the ongoing amplification process as it uses fluorescent reporter dyes that correlate PCR product concentration to fluorescence intensity, combining the steps of amplification and detection.

Reactions are characterized by the PCR cycle or point in time where the target amplification is first detected. This value is usually referred to as cycle threshold (Ct) and indicates the time at which fluorescence intensity is greater than background fluorescence. Consequently, the greater the quantity of target DNA in the starting material, the faster a significant fluorescent signal will appear, yielding a lower Ct.

PCR can be broken into phases: the linear ground phase, early exponential phase, log-linear (also known as exponential) phase, and plateau phase. During the first phase (usually the first 10–15 cycles), fluorescence emission at each cycle has not yet risen above background, so baseline fluorescence is calculated. At the early exponential phase, the amount of fluorescence has reached a threshold where it is significantly higher than background levels. Here is where Ct occurs, and it will be the value to calculate experimental results. After this phase, PCR reaches its optimal period where its product is doubled after every cycle in ideal conditions. Finally, the plateau stage is reached when reaction components become limited.

Among the types of real-time quantification, this study is based on comparative Ct method, which is a mathematical model that calculates changes in gene expression as a relative fold difference between an experimental and calibrator sample.

Real-time PCR results are commonly normalized against a control gene that may also serve as a positive control for the reaction. Ideally, the control gene should be expressed regardless of experimental conditions, like housekeeping genes are thought to be. Thus, GAPDH (Glyceraldehyde-3-Phosphate Dehydrogenase was chosen as the reference gene in this study.

First, murine specific primers for gene targets SphK1, SphK2, Atrogin-1 and P21, and for the housekeeping gene (GAPDH) were designed and used. The sequences of the primers are listed below.

GAPDH:	Forward (FW): 5′-GGCAAATTCAACGGCACAGTC 3′
	Reverse (RV): 5′ TCGCTCCTGGAAGATGGTG 3′
SphK1:	Forward: 5′ CTGGCAGCTTCTGTG AACCA 3’

	Reverse: 5′ TGTGCAGGGACAGCAGGTTCA 3′
SphK2:	Forward: 5′ GAACGACAGAACCATGCCC 3′
	Reverse: 5′ CTCGTAAAGCAGCCCGTCTC 3′
Atrogin-1:	Forward: 5′ GCAGCCAAGAAGAGAAAGAAA 3′
	Reverse: 5′ GCTGATAGCAAAGTCACAG 3′
P21:	Forward: 5′ CGAGAACGGTGGAACTTTGAC 3′
	Reverse: 5′ CAGGGCTCAGGTAGACCTTG 3′

For the amplification process, PCR Master Mix (Life Technologies, Carlsbad, CA, USA) kit was used. Reaction was prepared for each gene and sample in small loading tubes as follow indicated:

1) 1 µL of FW primer at 5 µM concentration
2) 1 µL of RV primers at 5 µM concentration
3) 22 µL of SYBR Green Master Mix (of which 10 µL are ddH_2O)
4) cDNA corresponding to 500ng, normally between 1-4 µL

The technology used was MIC qPCR cycler (Diatech Pharmacogenetics, Jesi, AN, Italy) and it carried out the following program: 95ºC for 10 min, 40 cycles at (95ºC for 30sec, T_m[1] for 30sec, 72ºC for 45sec), and a final step of 65-95ºC at 0,3ºC/sec.

[1]T_m for these genes vary between them so it is 52ºC for GAPDH (though it can work until 60ºC), 53ºC for Atrogin1, 57ºC for SK1, 59ºC for SK2 and 60ºC for P21. Note that it is not recommended to mix genes with different T_m as it could reduce efficiency.

Every experiment will be illustrated in a graphic like the one here showed in Figure 9, where a target gene (purple) is compared to a control sample (green). This way, it is possible to note anomalies in the logarithmic line of the course, which cannot be extracted from the numerical data and can indicate some kind of error.

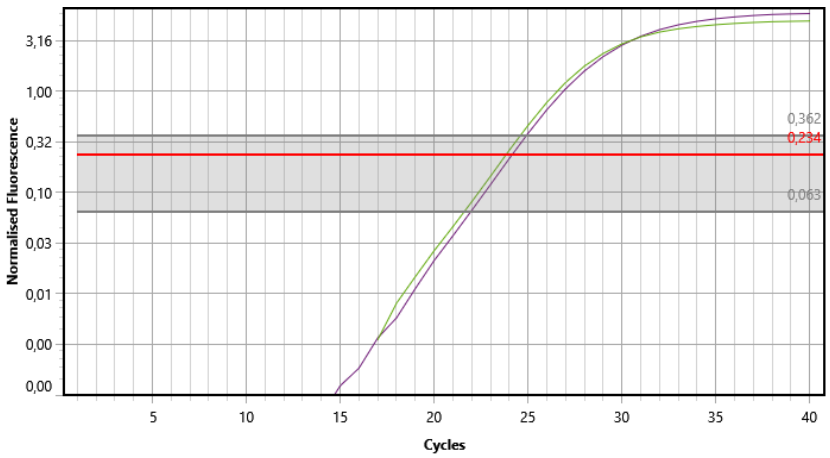

Figure 9. **Graphic given by MIC software after PCR course of one target and one control gene.** Ct correspond to the exact moment when the red line (fluorescence threshold) is crossed by the genes course (control gene represented in green and target gene in purple)

Relative SphK1, SphK2 transcript levels were calculated from the obtained data by the formulas specified in Fig. 10:

$$\Delta Ct = Ct_{target\ gene} - Ct_{housekeeping\ gene}$$

$$\Delta\Delta Ct = \Delta Ct - \Delta Ct_{reference}$$

$$fold = 2^{-\Delta\Delta Ct}$$

Figure 10. Statistic calculations to normalise data.

where ΔCt is the difference in Ct between the target gene and the housekeeping one, and the ΔΔCt is the difference between the ΔCt of the interest sample and the ΔCt of the reference one. Messenger RNA levels in control were arbitrarily set to 1.0. Fold refers to the log-ratio of a gene's or a transcript's expression values in two different conditions.

Representative table for the data of at least three independent experiments for each condition will appear within *Results*.

4. Results and discussion

Changes in C2C12 myoblasts after TSA exposure for SphK1, SphK2 and P21

Bioactive sphingolipids and their metabolizing enzymes represent interesting contribution to skeletal muscle atrophy. Among them, the SphK/S1P/S1PR axis has become quite interesting for its biological and therapeutic potential in cancer and inflammation. However, the complete pathway of this process it is yet to be understood.

It is well-known that post-translational modifications such as acetylation play important roles in the epigenetic regulation of gene expression. It has been noted that histone deacetylase class II is required to activate muscle atrophy as its involvement in the myogenin pathway induces the expression of E3 ubiquitin ligases atrophy-related, MuRF1 and Atrogin-1/MAFbx. The action of these HAT and HDAC enzyme also regulates the activity of FoxO family, very involved in muscle atrophy (Dupré-Aucouturier *et al.*, 2015).

Trichostatin A is an inhibitor of histone deacetylases, specifically HDAC1 and HDAC2. Previous studies have confirmed that this compound increases muscle cell size by promoting recruitment of myoblasts into myotubes. Furthermore, that process is unlikely to be dependant of IGF-1 pathway. The HDAC inhibitors seem to influence gene expression in a tissue-specific manner, activating follistatin expression in skeletal muscle (Iezzi *et al.*, 2004)

The data present in Table 2 showed that inhibitor TSA had a significant effect on decreasing SphK1 and SphK2 levels when comparing to healthy standards, appreciating sharper variations as longer the exposure was.

Equally, p21 appeared also to be downregulated after 48 hours of TSA exposure. This indicates that p21 expression is supressed, thus cell cycle is further activated to proliferation. Note that no effects were appreciated in the 24h-treated cells as no levels of expression were shown after PCR amplification, which may be caused because proliferation requires some time to be notable or due to some manipulating error as the experiment was performed just once n=1.

Overall, this may indicate that inhibiting histone deacetylase and thus inducing higher levels of acetylation promotes the activation/expression of a gene that can repress SphK1 and SphK2 expression and also p21, activating cell growth and proliferation towards differentiation into myotubes.

Changes in SphK1, SphK2 and Atrogin-1 levels in DEXA-induced atrophy and subsequent TSA treatment in C2C12 myotubes

In previous studies on the role of SphK/S1PRs axis in glucocorticoid-induced cachexia, it was reported that SphK1 did not suffer any significant variation while its active form (p-SphK1) was significantly decreased (Pierucci *et al.*, 2018). Here, it is noted that SphK1 increases significantly (fold > 6) in DEXA-treated myotubes. It may indicate its important role in skeletal muscle atrophy, but it will need more comparisons in next experiments.

Furthermore, the same previous study showed how SphK1 activity is necessary for counteracting Atrogin-1/MAFbx expression as it was overexpressed when treating the myotubes with an inhibitor of SphK1 activity. On the other hand, no significant variation on the atrophic protein

marker was appreciated when inhibiting SphK2 (Pierucci *et al.*, 2018). Although this was not proven in this study, DEXA-treated myotubes did show an outstanding increase in Atrogin-1 levels of expression being more its fold higher than 50, whereas SphK2 levels increased but were the less compromised. It is still clear that the glucocorticoids pathway is strongly related to muscle wasting.

Trichostatin A (TSA) has been demonstrated to restore skeletal muscle weight loss and normal muscle mass and fibre structure. Also, it has shown effects on inhibiting the upregulation of HDAC1/2 and ubiquitin degradation. Overall, it is well-known that TSA improves skeletal muscle atrophy condition trough HDAC inhibition, but the specific mechanisms are still to be discovered (Ding *et al.*, 2019).

In this experiment, the data obtained from exposing DEXA-treated myotubes to the inhibitor confirmed and detailed in Table 3 the mentioned improvement as it decreased successfully all the altered levels, although the initial basal expression in control myotubes was not achieved. Atrogin-1 represented the maximal variation compared to its expression rate shown after the treatment with DEXA (fold = 0,105). An equally decreasing result was obtained in both SphK1 and SphK2, but the effects caused by DEXA were not as elevated. However, the effects performed by TSA treatment made possible to conclude that HDAC activity is required for S1P pathways in skeletal muscle regulation, so epigenetics may have a key role in treating these conditions.

The effects of TSA treatment in C2C12 healthy myotubes were appreciated, concluding acetylation/deacetylation processes are key to muscle development. The data showed that SphK1 levels were overexpressed, while SphK2 had the opposite result. It may be caused by the well-known interaction between SphK2 with HDAC1/2 in the nucleus, although further investigation will be required. In addition, Atrogin-1 levels were also altered upwards, which may be a consequence of the imbalance in SphK1 and SphK2 normal pathways.

Myoblasts													
SphK1													
24 h													
			GAPDH				SphK1						
cDNA	Experiment		18th may	25th may	average	stand. dev.	18th may	25th may	average	stand. dev.	ΔCt	ΔΔCt	fold
1,5 microL	#1	control	16,31	15,94	16,125	0,26162951	23,68	23,98	23,83	0,21213203	7,705		**1**
		TSA 150 nM	16,63	16,51	16,57	0,08485281	24,22	24,01	24,115	0,14849242	7,545	-0,16	**1,11728714**
48 h													
			27th may	30th may			27th may	30th may					
4 microL	#3	control	13,31	13,3	13,305	0,00707107	20,96	21	20,98	0,02828427	7,675		1
		TSA 150 nM	13,21	13,2	13,205	0,00707107	22,42	22,4	22,41	0,01414214	9,205	1,53	**0,34627737**

SphK2													
24 h													
			GAPDH				SphK2						
cDNA	Experiment		18th may	25th may	average	stand. Dev.	18th may	25th may	average	stand. dev.	ΔCt	ΔΔCt	fold
1,5 microL	#1	control	16,31	15,94	16,125	0,26162951	22,61	22,6	22,605	0,00707107	6,48		1
		TSA 150 nM	16,63	16,51	16,57	0,08485281	23,46	23,5	23,48	0,02828427	6,91	0,43	**0,74226179**
48 h													
			27th may	30th may			27th may	30th may					
4 microL	#3	control	13,31	13,3	13,305	0,00707107	21,31	21,3	21,305	0,00707107	8		1
		TSA 150 nM	13,21	13,2	13,205	0,00707107	23,08	23	23,04	0,05656854	9,835	1,835	**0,28029152**

P21													
48 h													
			GAPDH				P21						
cDNA	Experiment		30th may	31st may	average	stand. Dev.	30th may	31st may	average	stand. dev.	ΔCt	ΔΔCt	fold
2 microL	#3	control	13,31	14,72	14,015	0,99702056	19,29	21,09	20,19	1,27279221	6,175		1
		TSA 150 nM	13,21	15,2	14,205	1,40714249	21,55	22,73	22,14	0,834386	7,935	1,76	**0,29524817**

Table 2. Variations on SphK1, SphK2 and P21 levels of expression compared to control culture in TSA-treated C2C12 myoblasts during 24 and 48 hours.

Myotubes (48 h)													
SphK1													
TSA													
			GAPDH				SphK1						
cDNA	Experiment		8th june	26th july	average	stand. dev.	8th june	26th july	average	stand. dev.	ΔCt	ΔΔCt	fold
1 microL	#1	control	13,76	18,37	16,065	3,25976226	19,83	26,54	23,185	4,7446865	7,12		1
		TSA 150 nM	15,41	19,54	17,475	2,92035101	19,91	26,93	23,42	4,9638896	5,945	-1,175	**2,25792881**
DEXA													
cDNA	Experiment		28th june	26th july	average	stand. dev.	28th june	26th july	average	stand. dev.	ΔCt	ΔΔCt	fold
1 microL	#1	control	13,76	18,37	16,065	3,25976226	19,83	26,54	23,185	4,7446865	7,12		1
		DEXA	13,44	16,64	15,04	2,2627417	20,53	18,24	19,385	1,61927453	4,345	-2,775	**6,84476021**
DEXA + TSA													
cDNA	Experiment		28th june	26th july	average	stand. dev.	28th june	26th july	average	stand. dev.	ΔCt	ΔΔCt	fold
1 microL	#1	DEXA	13,44	16,64	15,04	2,2627417	20,56	18,24	19,4	1,64048773	4,36		1
		DEXA + TSA	13,41	16,01	14,71	1,83847763	21,16	22,61	21,885	1,02530483	7,175	2,815	**0,14210212**

SphK2													
TSA													
			GAPDH				SphK2						
cDNA	Experiment		7th july	25th july	average	stand. dev.	7th july	25th july	average	stand. dev.	ΔCt	ΔΔCt	fold
1 microL	#1	control	17,36	17,45	17,405	0,06363961	26,36	26,29	26,325	0,04949747	8,92		1
		TSA 150 nM	15,32	19,31	17,315	2,82135606	24,45	28,46	26,455	2,83549819	9,14	0,22	**0,85856544**
DEXA													
cDNA	Experiment		7th july	25th july	average	stand. dev.	7th july	25th july	average	stand. dev.	ΔCt	ΔΔCt	fold
1 microL	#1	control	17,36	17,45	17,405	0,06363961	26,36	26,29	26,325	0,04949747	8,92		1
		DEXA	15,44	16,64	16,04	0,84852814	23,51	24,51	24,01	0,70710678	7,97	-0,95	**1,93187266**
DEXA + TSA													
cDNA	Experiment		28th june	25th july	average	stand. dev.	28th june	25th july	average	stand. dev.	ΔCt	ΔΔCt	fold
1 microL	#1	DEXA	13,44	16,64	15,04	2,2627417	23,54	24,51	24,025	0,68589358	8,985		1
		DEXA + TSA	13,41	15,32	14,365	1,35057395	23,45	23,61	23,53	0,11313708	9,165	0,18	**0,882703**

Atrogin-1													
TSA													
			GAPDH				Atrogin-1						
cDNA	Experiment		8th june	26th july	average	stand. dev.	8th june	26th july	average	stand. dev.	ΔCt	ΔΔCt	fold
1 microL	#1	control	14,41	18,37	16,39	2,80014285	22,17	24,56	23,365	1,68998521	6,975		1
		TSA 150 nM	15,91	19,54	17,725	2,56679762	21,66	23,73	22,695	1,46371104	4,97	-2,005	**4,01388699**
DEXA													
cDNA	Experiment		17th june	27th july	average	stand. dev.	17th june	27th july	average	stand. dev.	ΔCt	ΔΔCt	fold
1 microL	#1	control	18,83	14,41	16,62	3,12541197	24,38	22,17	23,275	1,56270599	6,655		1
		DEXA	19	13,44	16,22	3,9315137	19,09	15,19	17,14	2,75771645	0,92	-5,735	**53,260719**
DEXA + TSA													
cDNA	Experiment		27th june	17th july	average	stand. dev.	27th june	17th july	average	stand. dev.	ΔCt	ΔΔCt	fold
1 microL	#1	DEXA	13,44	19,1	16,27	4,00222438	15,19	19,09	17,14	2,75771645	0,87		1
		DEXA + TSA	13,41	16,06	14,735	1,87383297	17,66	20,05	18,855	1,68998521	4,12	3,25	**0,10511205**

Table 3. Variations on SphK1, SphK2 and Atrogin-1 levels of expression compared to control culture in C2C12 myotubes treated with TSA, DEXA and both 48 hours.

5. Conclusions and future perspective

The fact that histone deacetylation inhibition, thus acetylation persistence, does not result in a major different in SphK1 and SphK2 levels of expression, while the results of TSA treatment to cells DEXA-induced to cachexia represent an appreciable improvement; leads us to conclude that HAT/HDAC pathways have an important role in S1P/S1PR axis. However, it is still necessary to further investigate the specific role of all these molecules to understand the mechanisms behind the improvements shown after TSA treatment.

As future projection of this study, some experiments I would suggest would involve:

- The differential expression of S1P receptors in the conditions here shown (control, TSA, DEXA and DEXA + TSA)
- Variations in other components of the S1P/S1PR axis, such as CERK
- Altered expression of other E3 ligases like MuRF1 or MUSA1
- Multiple verifications of these results with a higher number of experiments variating concentration or exposure

6.- References

1. Bonaldo, P., & Sandri, M. (**2013**). Cellular and molecular mechanisms of muscle atrophy. Disease models & mechanisms, 6(1), 25–39.
2. Schiaffino, S., Dyar, K. A., Ciciliot, S., Blaauw, B., & Sandri, M. (**2013**). Mechanisms regulating skeletal muscle growth and atrophy. The FEBS journal, 280(17), 4294–4314.
3. Cohen, S., Nathan, J. A., & Goldberg, A. L. (**2015**). Muscle wasting in disease: molecular mechanisms and promising therapies. Nature reviews. Drug discovery, 14(1), 58–74.
4. Larsson, L., Degens, H., Li, M., Salviati, L., Lee, Y. I., Thompson, W., Kirkland, J. L., & Sandri, M. (**2019**). Sarcopenia: Aging-Related Loss of Muscle Mass and Function. Physiological reviews, 99(1), 427–511.
5. Fearon, K., Strasser, F., Anker, S. D., Bosaeus, I., Bruera, E., Fainsinger, R. L., Jatoi, A., Loprinzi, C., MacDonald, N., Mantovani, G., Davis, M., Muscaritoli, M., Ottery, F., Radbruch, L., Ravasco, P., Walsh, D., Wilcock, A., Kaasa, S., & Baracos, V. E. (**2011**). Definition and classification of cancer cachexia: an international consensus. The Lancet. Oncology, 12(5), 489–495.
6. Argilés, J. M., Busquets, S., Stemmler, B., & López-Soriano, F. J. (**2014**). Cancer cachexia: understanding the molecular basis. Nature reviews. Cancer, 14(11), 754–762.
7. Argilés, J. M., Busquets, S., & López-Soriano, F. J. (**2019**). Cancer cachexia, a clinical challenge. Current opinion in oncology, 31(4), 286–290.
8. Lira, F. S., Antunes, B., Seelaender, M., & Rosa Neto, J. C. (**2015**). The therapeutic potential of exercise to treat cachexia. Current opinion in supportive and palliative care, 9(4), 317–324.
9. Sandri M. (**2016**). Protein breakdown in cancer cachexia. Seminars in cell & developmental biology, 54, 11–19.
10. Yin, L., Li, N., Jia, W., Wang, N., Liang, M., Yang, X., & Du, G. (**2021**). Skeletal muscle atrophy: From mechanisms to treatments. Pharmacological research, 172, 105807.
11. Roux, P. P., & Topisirovic, I. (**2012**). Regulation of mRNA translation by signaling pathways. Cold Spring Harbor perspectives in biology, 4(11), a012252.
12. Bodine, S. C., & Furlow, J. D. (**2015**). Glucocorticoids and Skeletal Muscle. Advances in experimental medicine and biology, 872, 145–176.
13. Menconi, M., Fareed, M., O'Neal, P., Poylin, V., Wei, W., & Hasselgren, P. O. (**2007**). Role of glucocorticoids in the molecular regulation of muscle wasting. Critical care medicine, 35(9 Suppl), S602–S608.
14. Schakman, O.; Kalista, S.; Barbé, C.; Loumaye, A.; Thissen, J.P. (**2013**). Glucocorticoid-induced skeletal muscle atrophy. The International Journal of Biochemistry & Cell Biology, 45(10), 2163–2172.
15. Olivera, A., Allende, M. L., & Proia, R. L. (**2013**). Shaping the landscape: metabolic regulation of S1P gradients. Biochimica et biophysica acta, 1831(1), 193–202.
16. Cordeiro, A. V., Silva, V., Pauli, J. R., da Silva, A., Cintra, D. E., Moura, L. P., & Ropelle, E. R. (**2019**). The role of sphingosine-1-phosphate in skeletal muscle: Physiology, mechanisms, and clinical perspectives. Journal of cellular physiology, 234(7), 10047–10059.

17. Meacci, E., Nuti, F., Donati, C., Cencetti, F., Farnararo, M., & Bruni, P. (**2008**). Sphingosine kinase activity is required for myogenic differentiation of C2C12 myoblasts. Journal of cellular physiology, 214(1), 210–220.
18. Sassoli, C., Frati, A., Tani, A., Anderloni, G., Pierucci, F., Matteini, F., Chellini, F., Zecchi Orlandini, S., Formigli, L., & Meacci, E. (**2014**). Mesenchymal stromal cell secreted sphingosine 1-phosphate (S1P) exerts a stimulatory effect on skeletal myoblast proliferation. PloS one, 9(9), e108662.
19. Pierucci, F., Frati, A., Battistini, C., Matteini, F., Iachini, M. C., Vestri, A., Penna, F., Costelli, P., & Meacci, E. (**2018**). Involvement of released sphingosine 1-phosphate/sphingosine 1-phosphate receptor axis in skeletal muscle atrophy. Biochimica et biophysica acta. Molecular basis of disease, 1864(12), 3598–3614.
20. Meacci, E., & Garcia-Gil, M. (**2019**). S1P/S1P Receptor Signaling in Neuromuscolar Disorders. International journal of molecular sciences, 20(24), 6364.
21. Fernández, A.B. (**2014**). Las HDAC en la regulación de la expresión génica y el cáncer.
22. Carrozza, M. J., Utley, R. T., Workman, J. L., & Côté, J. (2003). The diverse functions of histone acetyltransferase complexes. Trends in genetics, TIG, 19(6), 321–329.
23. Beharry, A. W., & Judge, A. R. (**2015**). Differential expression of HDAC and HAT genes in atrophying skeletal muscle. Muscle & nerve, 52(6), 1098–1101.
24. Renzini, A., D'Onghia, M., Coletti, D., & Moresi, V. (**2022**). Histone Deacetylases as Modulators of the Crosstalk Between Skeletal Muscle and Other Organs. Frontiers in physiology, 13, 706003.
25. Dupré-Aucouturier, S., Castells, J., Freyssenet, D., & Desplanches, D. (**2015**). Trichostatin A, a histone deacetylase inhibitor, modulates unloaded-induced skeletal muscle atrophy. Journal of applied physiology (Bethesda, Md, 1985), 119(4), 342–351.
26. Hagiwara, H., Saito, F., Masaki, T., Ikeda, M., Nakamura-Ohkuma, A., Shimizu, T., & Matsumura, K. (**2011**). Histone deacetylase inhibitor trichostatin A enhances myogenesis by coordinating muscle regulatory factors and myogenic repressors. Biochemical and biophysical research communications, 414(4), 826–831.
27. Ding, J., Li, F., Cong, Y., Miao, J., Wu, D., Liu, B., & Wang, L. (**2019**). Trichostatin A inhibits skeletal muscle atrophy induced by cigarette smoke exposure in mice. Life sciences, 235, 116800.
28. Guo, K., Wang, J., Andrés, V., Smith, R. C., & Walsh, K. (**1995**). MyoD-induced expression of p21 inhibits cyclin-dependent kinase activity upon myocyte terminal differentiation. Molecular and cellular biology, 15(7), 3823–3829.
29. Iezzi, S., Di Padova, M., Serra, C., Caretti, G., Simone, C., Maklan, E., Minetti, G., Zhao, P., Hoffman, E. P., Puri, P. L., & Sartorelli, V. (**2004**). Deacetylase inhibitors increase muscle cell size by promoting myoblast recruitment and fusion through induction of follistatin. Developmental cell, 6(5), 673–684.